Carbon screen-printed electrodes on ceramic substrates for label-free molecular detection of antibiotic resistance

Obaje, Eleojo; Cummins, Gerard; Schulze, Holger; Mahmood, Salman; Desmulliez, Marc Phillipe Yves; Bachmann, Till

DOI:
10.1002/jin2.16

Document Version
Publisher's PDF, also known as Version of record

Citation for published version (Harvard):
Obaje, E, Cummins, G, Schulze, H, Mahmood, S, Desmulliez, MPY & Bachmann, T 2016, 'Carbon screen-printed electrodes on ceramic substrates for label-free molecular detection of antibiotic resistance', *Journal of Interdisciplinary Nanomedicine*, vol. 1, no. 3, pp. 93-109. https://doi.org/10.1002/jin2.16

Journal of
Interdisciplinary Nanomedicine

BRITISH SOCIETY FOR NANOMEDICINE

Open Access

Journal of Interdisciplinary Nanomedicine ISSN 2058-3273

ORIGINAL ARTICLE

Carbon screen-printed electrodes on ceramic substrates for label-free molecular detection of antibiotic resistance

Eleojo A. Obaje[1] Gerard Cummins[2] Holger Schulze[1] Salman Mahmood[2] Marc P.Y. Desmulliez[2] & Till T. Bachmann[1*]

[1] *Division of Infection and Pathway Medicine, Edinburgh Medical School, College of Medicine and Veterinary Medicine, The University of Edinburgh, Chancellor's Building, 49 Little France Crescent, Edinburgh EH16 4SB, Scotland, UK*

[2] *School of Engineering and Physical Sciences, MIcroSystems Engineering Centre, Heriot-Watt University, Edinburgh EH14 4AS, Scotland, UK*

Keywords
Antimicrobial resistance, bla_{NDM}, carbon electrodes, DNA binding, electrochemical impedance spectroscopy, Low Temperature Co-fired Ceramic, New Delhi metallo-beta-lactamase, point of care, sensor.

Correspondence
Till T. Bachmann, Division of Infection and Pathway Medicine, Edinburgh Medical School, College of Medicine and Veterinary Medicine, The University of Edinburgh, Chancellor's Building, 49 Little France Crescent, Edinburgh EH16 4SB, Scotland, UK.
Tel: +44 131 242 9437;
fax: +44 131 242 6244;
E-mail: Till.Bachmann@ed.ac.uk

FUNDING INFORMATION
Scottish Innovation Centre for Sensor and Imaging Systems20130219_Molnlycke

Received: 24 March 2016;
Revised: 22 June 2016;
Accepted: 20 July 2016

Journal of Interdisciplinary Nanomedicine, 2016; 1(3), doi: 10.1002/jin2.16

Abstract

The growing threat posed by antimicrobial resistance on the healthcare and economic well-being of mankind is pushing the need to develop novel and improved diagnostic platforms for its rapid detection at point of care, facilitating better patient management strategies during antibiotic therapy. In this paper, we present the manufacturing and characterisation of a low-cost carbon screen-printed electrochemical sensor on a ceramic substrate. Using label-free electrochemical impedance spectroscopy, the sensor is demonstrated for the detection of bla_{NDM}, which is one of the main antimicrobial resistance factors in carbapenem-resistant Enterobacteriaceae. The electrochemical performance of the newly fabricated sensor was initially investigated in relation to the function of its underlying composite materials, evaluating the choice of carbon and dielectric pastes by characterising properties like surface roughness, wetting and susceptibility of unspecific DNA binding. Subsequently, the sensor was used in an electrochemical impedance spectroscopy assay for the sensitive and specific detection of synthetic bla_{NDM} targets achieving a detection limit of 200 nM. The sensor properties and performance demonstrated in this study proved the suitability of the new electrode materials and manufacturing for further point-of-care test development as an inexpensive and effective alternative to gold electrodes sensor.

Introduction

Antimicrobial resistance (AMR) is one of the greatest healthcare challenges that mankind is facing. AMR has been recognised as a global public health issue, with substantial societal and economic impacts with around 10 million deaths annually by 2050 and gross domestic product losses of $100 trillion estimated if AMR is not tackled. (O'Neill, 2014) Novel diagnostics are expected to reduce the number of inappropriate prescriptions of antibiotics for the benefit of patients. In that respect, molecular diagnostics can give quick results, determine the AMR mechanism and be performed at point of care (POC). There is international consensus that carbapenemase-producing Enterobacteriaceae is a critical and urgent AMR threat because of their rapidly increasing prevalence, high associated mortality rates, and severely limited treatment options. (CDC, 2013; ECDC, 2011) The species among the Enterobacteriaceae, where carbapenem resistance is of greatest relevance, are *Escherichia coli* (*E. coli*) and *Klebsiella (K.)* pneumonia which can obtain their resistance by acquiring genes for carbapenem hydrolysing enzymes, with KPC (*Klebsiella pneumoniae* carbapenemase), NDM (New Delhi metallo-beta-lactamase), IMP, VIM, OXA-48 being considered as the Big 5 of carbapenemases. (Hawkey, 2015; Temkin et al., 2014) In that regard, the bla_{NDM} gene encoding for the NDM beta-lactamase has been identified with having a critical role because organisms containing bla_{NDM} tend to be multiresistant and are only sensitive to the last option treatments like tigecycline and colistin, which have uncertain efficacies. (Kumarasamy et al., 2010) Although bla_{NDM} was originally identified in *E. coli* and *K.* strains, it has now been observed in many Enterobacteriaceae, which are responsible for a range of infections including sepsis and urinary tract infections. Additionally, the gene is easily transmitted horizontally between Gram-negative bacteria. (Fomda et al., 2014; Jean et al., 2015; Nordmann, 2010) Consequently, rapid identification of NDM strains is of critical importance to prevent the accelerated circulation of resistant strains.

Presently, most of the available diagnostic approaches for the detection of extended-spectrum beta-lactamase (ESBL) and carbapenemase producing bacteria are culture-based, with unacceptable time-to-results for effective therapeutic management. (Carrer et al., 2010; Farber et al., 2008; Linscott and Brown, 2005; Reglier-Poupet et al., 2008) Such diagnostic approaches include ChromID ESBL, Etest ESBL, and Vitek (bioMerieux). Additionally, there are commercially available solutions for the molecular detection of beta-lactam resistance in Gram-negative bacteria, like Check-MDR (Checkpoints), Evigene (AdvanDx), Hyplex SuperBug ID (Amplex); however, these are all based on complex optical readout systems and are not suitable for POC detection as they also require demanding sample preparation and pre-analytics. (Fosheim et al., 2007; Kaase et al., 2012; Naas et al., 2011) Therefore, electrochemical biosensors provide unique opportunities to develop suitable POC devices for better clinical diagnostics due to their specificity and speed of the detection technique, as well as the portability and low cost of the sensors. This paper describes the fabrication, characterisation, and functionalisation of a carbon-based impedimetric electrochemical sensor for molecular diagnostics in such POC application.

Electrochemical Impedance Spectroscopy and Electrochemical Sensors

Electrochemical impedance spectroscopy (EIS) is a technique that can be utilised to observe biorecognition events on functionalised electrode surfaces. (Ciani et al., 2012; Corrigan et al., 2012; Corrigan et al., 2013; Gebala et al., 2009; Huang et al., 2015; Kafka et al., 2008; Lisdat and Schäfer, 2008; Witte and Lisdat, 2011) The detection of DNA hybridisation events using EIS is a growing field of study and has been covered extensively in review articles. (Cederquist and Kelley, 2012; Lindholm-Sethson et al., 2010; Lisdat and Schäfer, 2008; Park and Park, 2009; Suginta et al., 2013) In general, nucleic acid probes are functionalised onto an electrode surface, which has been so far mainly, if not exclusively, a gold electrode surface, forming a mixed self-assembled monolayer (SAM). In the case of Faradaic EIS as illustrated in Figure 1B, measurements are performed in the presence of a soluble redox mediator such as potassium ferric ferrocyanide, for example. DNA strand hybridising to probes result in the accumulation of negative charges on the electrode surface, and an increase in the charge transfer resistance (R_{CT}) of the system is measured. This increase can be explained by the repulsion of anionic redox mediators at the electrode surface combined with the blocking of SAM pinholes by a bound complementary DNA target, thereby inhibiting the electron transfer process. (Corrigan et al., 2012) EIS therefore lends itself well to multiplex detection within an electrode array, whereby multiple markers of infection and resistance may be evaluated in parallel.

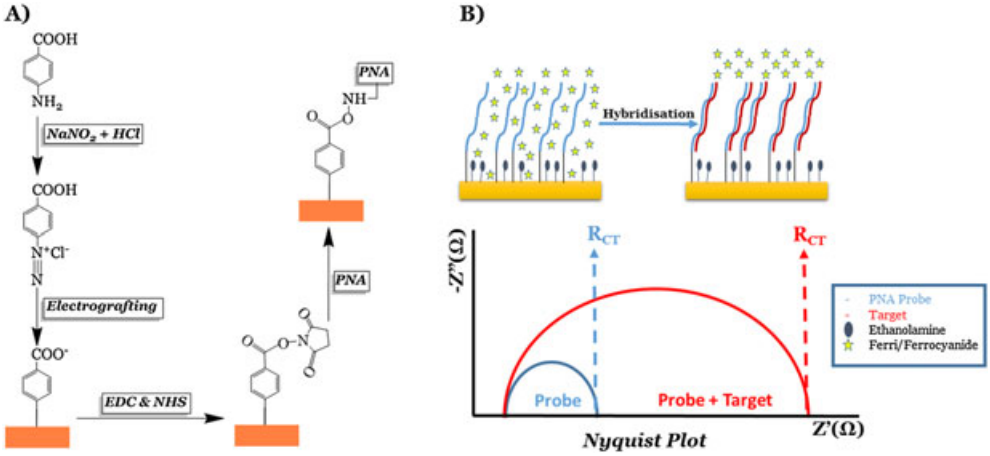

Figure 1. (A) Carboxyphenyl modification of the carbon electrode surface and the covalent immobilisation of peptide nucleic acid (PNA) probes. (B) Working principle of the detection assay via electrochemical impedance spectroscopy.

Electrochemical sensors can be monolithically manufactured by depositing onto a substrate of one or more conductive layers to form the working, counter and reference electrodes and a dielectric layer to protect these electrodes from the surrounding environment. This structure can be easily achieved without resorting to more traditional and expensive microfabrication techniques such as photolithography, sputtering, and etching. One method already widely used to rapidly produce inexpensive electrochemical sensors is screen printing. (Grieshaber et al., 2008) A less common manufacturing method for such sensors uses Low Temperature Co-fired Ceramics (LTCC) technology. (Lacrotte et al., 2013) LTCC are glass-ceramic composite materials which have been used over the last 20 years in the production of electronic packages and multi-chip modules for harsh environment applications found in the oil and gas and automotive sectors, for example. Recent material advances enabling self-constrained LTCC layers have enabled the successful manufacturing of microsystems devices as an alternative to more traditional materials such as glass, polymers, and silicon as LTCC manufacturing does not require the use of expensive cleanrooms, photolithographic patterning, or corrosive chemicals. Furthermore, LTCC has a number of properties such as high temperature stability, chemical inertness, biocompatibility, and mechanical strength that are desirable for POC diagnostic applications. LTCC usually comes in the form of a tape made of a ceramic filler (usually alumina, Al_2O_3), a glass frit enabling lower processing temperatures of the order of 870 °C and organic components such as solvent, plasticizer, and binder. The tape is available in various thicknesses ranging from 100 to 400 μm. In their unfired state, these tapes are malleable which permits low cost machining to feature sizes ranging from 10 μm to 10 mm. (Gongora-Rubio et al., 2001; Ibáñez-García et al., 2008; Vasudev et al., 2013; Wilhelm et al., 2012)

The relatively low firing temperature of LTCC enables working metals such as gold, silver, and copper to be used. These metals can be easily deposited using the screen-printing process. (Kay and Desmulliez, 2012) This property is especially important for the fabrication of the electrochemical sensor electrodes, where metals such as gold and silver are widely used. Silver is widely used to produce an inexpensive and stable Ag/AgCl reference electrode using various chlorination methods. Gold is often used as a working or counter electrode as many surface chemistries required to immobilise various antibodies, enzymes, or mediator molecules on this metal are well documented. Although gold is expensive, it is widely used for its biocompatibility and lack of oxidation.

In this work, carbon pastes have been used to form the counter and working electrodes. Carbon pastes are attractive for most sensing applications because of their low cost, low background currents, and broad potential windows. (Wang et al., 1996; Wang et al., 1998) The exact composition of many commercially available pastes is unknown as it is considered proprietary information. Differences in composition, curing, and other processing conditions can significantly affect the performance of the fabricated electrochemical sensors. The effect of these parameters on the behaviour of our sensors is investigated in this article along with other factors such as the wetting and susceptibility of the dielectric layer to unspecifically bind target DNA.

Additionally as illustrated in Figure 1A, a probe functionalisation protocol for the immobilisation of peptide nucleic acid (PNA) probes on carbon electrodes has been developed and characterised in this article by evaluating its ability to be used in a functional EIS assay to detect a bla_{NDM} gene constructs in comparison with the current research on EIS.

Materials and Methods

Reagents

Deoxyribonucleic acid oligonucleotides were purchased from Metabion (Martinsried, Germany). PNA oligonucleotides were ordered via Cambridge Research Biochemicals (Cleveland, UK) from Panagene (Daejeon, South Korea). Potassium ferricyanide, potassium ferrocyanide, phosphate buffered saline buffer (10 mM, pH 7.4), monosodium phosphate, disodium phosphate, potassium chloride, 4-Aminobenzoic acid, sodium chloride, sodium nitrite ($NaNO_2$), hydrochloric acid, 2-(N-morpholino) ethanesulfonic acid (MES), ethanolamine, 1-Ethyl-3-(3-dimethylaminopropyl) carbodiimide hydrochloride (EDC) and N-hydroxysuccinimide (NHS) were purchased from Sigma-Aldrich (Poole, UK). A MES buffer solution (100 mM, pH 5.0) was used in the activation of the carboxylic groups. All solutions were prepared using deionised water ($>18\,M\Omega\,cm$).

Fabrication of screen-printed electrodes

The three-electrode system consists of a reference, working, and counter electrode. The silver reference electrode interconnects carbon counter and working electrodes and dielectric layers are defined using separate screen designs (DEK Stencils, ASM Assembly Systems, Munich, Germany). The structure of the device is shown in Figure 2. The screens can be used to simultaneously produce 12 electrochemical sensors.

The three-electrode system was fabricated on a LTCC substrate. This can be easily shaped in the green tape form and is mechanically rigid and chemical inert once fired. Multiple 72-mm-wide squares of LH2000 LTCC tape (Heraeus, Hanau, Germany) were cut using an Epilog Mini 18 40 W CO_2 laser (Epilog, CO, USA).

Several of these squares were coated with a single layer of Heraeus TC 7304 silver via paste using a DEK Horizon 03i screen-printer (ASM Assembly Systems, Munich, Germany). The deposited paste defined the reference electrode, and the electrical interconnects between the external potentiostat and the electrochemical sensor. All pastes were printed with the parameters shown in Table 1.

As the thickness of the LTCC sheets is reduced during firing, it was necessary to align and stack the printed LTCC films with five uncoated films in order to get the desired 500 μm substrate thickness such that the resulting electrodes can be connected to potentiostats via commercially available connectors such as the Dropsens box connectors (Dropsens, Oviedo, Spain). These layers were mechanically aligned using a stainless steel rig before being hermetically sealed in vacuum packed foil bags to withstand immersion in a Keko ILS-4 isostatic press (Keko Equipment, Žužemberk, Slovenia). The hydrostatic pressure generated by the press, and the 70 °C ambient temperature forces the individual layers to start fusing with one another and ensure the strength of the final structure. After compression, the LTCC stack is removed from the foil bag and mechanical jig and fired in a furnace. The firing

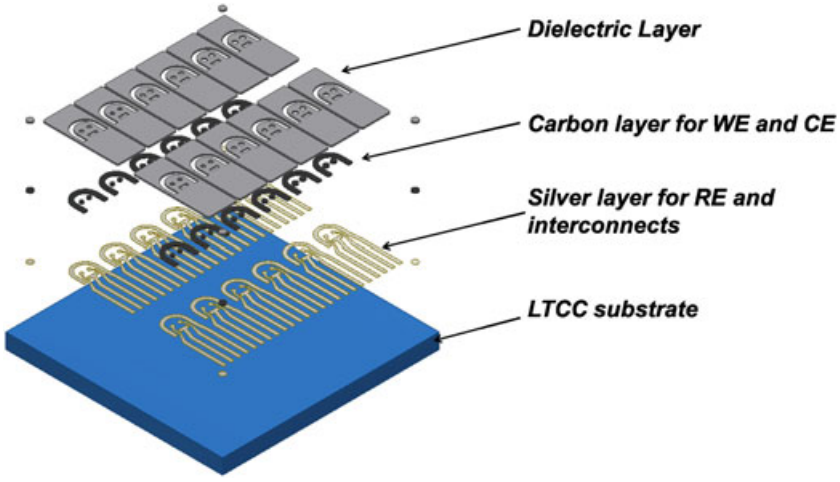

Figure 2. Exploded view of the screen-printed carbon electrode structure.

Table 1. Screen-printing parameters.

Parameter	Value
Front and rear squeegee pressure	4 kg
Front and rear speed	5 mms^{-1}
Separation speed	17 mms^{-1}
Separation distance	1 mm
Print gap	1.5 mm

process consists of two stages. First, the temperature in the furnace is ramped up to 450 °C from room temperature over a period of 7 h. The temperature is maintained at 450 °C for 45 min to ensure that all the organic components are burned out. The second part of the firing process involves increasing the temperature to 870 °C for 90 min. The LTCC stack is held at this temperature for 30 min before being slowly cooled back down to room temperature. During this second stage, the glass frit within the LTCC tape melts enabling the alumina particles to penetrate between adjacent layers of tape, thereby increasing the mechanical rigidity and strength of the final structure.

The working and counter electrodes of the sensor were printed using BQ242, BQ221, and 7105 carbon pastes from DuPont (DuPont, Delaware, USA) to determine which one had the best electrochemical response and easiest functionalisation property. Each carbon paste was printed on top of an underlying silver contact using the same printing process as before. After curing the carbon, an insulating layer was printed to protect the silver interconnects from the external environment while allowing the electrodes to be exposed to external analytes. The insulating pastes (D2071120D1, D2070423D5, and D2020823P2) from Gwent (Gwent Electronic Materials Ltd, Pontypool, UK) were printed using the DEK Horizon printing equipment and cured at 130 °C for 15 min under ambient atmosphere in a covered hotplate. The dielectric pastes were assessed in terms of hydrophobicity and their susceptibility to unspecific DNA binding.

The LTCC plates were singulated using a Disco DAD-640 dicing tool (Disco Corporation, Tokyo, Japan) to separate the individual electrochemical sensors for testing. A series of printed carbon electrodes on a nonsingulated LTCC plate is shown in Figure 3.

Characterisation of low temperature co-fired ceramic carbon pastes

The different carbon electrodes produced with three different DuPont carbon pastes (BQ242, BQ221, and 7105) were electrochemically characterised with an Autolab PGSTAT12 potentiostat (Metrohm Autolab, Herisau, Switzerland) by recording cyclic voltammograms (CV) in the presence of the redox pair 10 mM Ferri/Ferrocyanide ($Fe[CN]_6^{3-/4-}$) in phosphate buffer (100 mM sodium phosphate with 200 mM NaCl, pH 7.4) at 50 $mV\,s^{-1}$ scan rate. The samples were beforehand chronoamperometrically cleaned by applying a fixed potential of 1.5 V for 120 s in the presence saturated Na_2CO_3 solution. (Pesquero et al., 2013) Oxidation and reduction peak potentials during the scans were examined to determine the peak separation (ΔE_p) of the

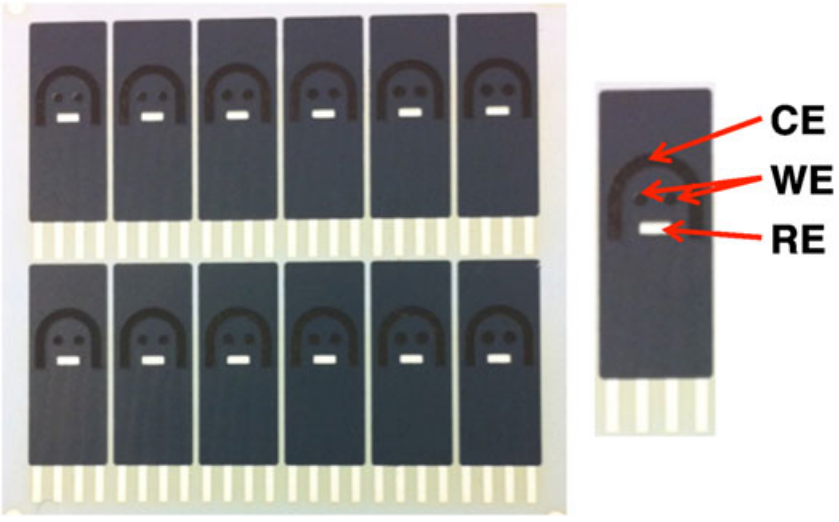

Figure 3. Electrochemical screen-printed carbon electrode sensors on non-singulated Low Temperature Co-fired Ceramics plate. Screen-printed carbon electrode sensors are shown to have two working (WE), and a counter electrode (CE) made out of carbon with a silver reference electrode (RE).

redox couple and used as a measure of the quality of electrodes surface. These LTCC carbon pastes were compared with commercially available Dropsens DRP-C1110 screen-printed carbon electrodes (Dropsens, Oviedo, Spain). The structure of the screen-printed films generated by the chosen carbon paste were also investigated by scanning electron microscopy and surface profilometry using a FEI Quanta 3D FEG system (FEI, OR, USA) and Dektak 3 (Bruker, MA, USA), respectively.

Characterisation of the dielectric materials

Three different Gwent dielectric insulation materials (D5, D1, and P2) were tested in terms of unspecific DNA binding and hydrophobicity of the dielectric surface. Both factors are important when immobilising and attaching analytical probes such as PNA to the electrode surface.

For contact angle measurements, samples were initially wiped with IsoPropyl Alcohol, and measurements were taken at different spots on the samples using droplets of deionised water. Droplet images were taken using the FTA32 software (First Ten Angstroms, VA, USA) with a custom made goniometer at the Scottish Microelectronics Centre, Edinburgh, UK. Contact angle was measured using the Dropsnake ImageJ plugin developed by the Biomedical Imaging Group at Ecole Polytechnique Federal de Lausanne (EPFL), Switzerland.

Additionally, evaluation of unspecific binding of Cy3-labelled DNA oligonucleotides to different dielectric materials was undertaken. Cy3-labelled DNA oligonucleotides used at varying concentrations and lengths were dissolved in 2x saline sodium citrate buffer (SSC; 300 mM sodium chloride + 30 mM sodium citrate) and incubated on the different dielectric surfaces for 30 min using 25 μL Gene Frames (Thermo Fisher Scientific), followed by rinsing with 2x SSC and deionised water. After drying the dielectric samples with Argon, fluorescence images were generated with a Tecan LS Reloaded fluorescence scanner (Tecan, Maennedorf, Switzerland) with excitation at 532 nm and emission at 575 nm at PMT 70 chosen to maximise signal without pixel saturation.

Functionalisation of the LTCC carbon electrodes with *bla*$_{NDM}$ specific PNA probes

Screen-printed carbon electrode sensors (SPCEs) were functionalised with amino-modified PNA probes (*bla*$_{NDM}$ variant) by electrografting via in situ generated diazonium cations from an in-house modified protocol. (Eissa and Zourob, 2012) Initially, diazonium cations were generated in situ by mixing 2 mM $NaNO_2$ solution with 2 mM 4-aminobenzioc acid in 0.5 M HCl. The electrochemical modification of SPCE was then performed by the reduction of the in situ generated 4-carboxyphenyl diazonium salt (4-CPDS) using four cyclic voltammetry scans from +0.4 to −0.6 V at a scan rate of 100 mV s^{-1} creating a 4-carboxyphenyl (AP) film on the electrode surface. The electrode was then washed thoroughly with water. The AP film on the electrode surface was activated by incubation with 250 mM EDC and 50 mM NHS (unless specified otherwise) in 100 mM MES buffer (pH 5.0) for about 60 min. Following this, the modified electrode surface was rinsed in MES buffer and then covered with a 50 μL droplet of 20 μM amino-modified PNA probe in PBS buffer, (10 mM phosphate, 150 mM sodium chloride pH 7.4) and incubated for 60 min at room temperature in a water-saturated atmosphere. Optimal probe concentrations for the assay sensitivity were also evaluated. The electrode surface was then washed with PBS (pH 7.4), blocked by adding 50 μL blocking buffer (1% v/v) ethanolamine in PBS buffer (pH 7.4), and incubated for 30 min in water-saturated atmosphere to deactivate the remaining active groups and to block the free surface. The modified electrode was then rinsed with PBS and dried under argon prior to use in the EIS assay.

Electrochemical impedance spectroscopy measurements

Following functionalization of the surface, EIS measurements were performed on SPCEs connected to an Autolab PGSTAT12 potentiostat controlled by Nova software (www.metrohm-autolab.com) at open circuit potential at an amplitude of 10 mV rms at 20 frequencies in the range between 100,000 and 0.3 Hz. Hybridisation and measurements were performed in 1 mM KCl with 2 mM $Fe[CN]_6^{3-/4-}$ unless stated otherwise. EIS response was also compared with a functionalised Dropsens SPCE DRP-C1110, and EIS measurements were also used to characterise each functionalisation step.

For the EIS assay characterisation, a previously designed *bla*$_{NDM}$ specific, amino-modified PNA probe (20 mer) was used to target a complementary synthetic 20 nucleotide long DNA oligonucleotide (Huang et al., 2015), and the assay response was compared between fabricated LTCC SPCE and the commercially available Dropsens SPCE. Additionally, the specificity of the assay was measured against a noncomplementary synthetic

DNA sequence (27 mer). Table 2 in the following discussions shows the sequences used in the EIS assay. Furthermore, the overall assay sensitivity of the functionalised LTCC SPCE was also evaluated against a recently published paper that used EIS to target the same *bla*$_{NDM}$ gene constructs (i.e., with the same PNA probes and synthetic DNA targets) but were functionalised on Dropsens gold electrodes. (Huang et al., 2015)

Results and Discussion

Effect of the carbon paste

In developing a novel SPCEs, the various carbon pastes and dielectric materials were evaluated to characterise the functions of its underlying components. SPCEs produced with each of the different DuPont carbon pastes (BQ242, BQ221, and 7105) were cured at 130 °C for 15 min under ambient atmosphere and electrochemically characterised by recording CVs in $Fe[CN]_6^{3-/4-}$ (scan rate 50 mV s^{-1}), after chronoamperometric cleaning in saturated Na_2CO_3 solution. The ΔE_p values were evaluated and compared with that of a commercially available Dropsens DRP-C1110 SPCE. Figure 4 shows a graphical representation of the recorded ΔE_p values, which are a measure for the quality of the electrodes surface. Carbon paste BQ242 was observed to perform best with a ΔE_p of 119 ± 10.5 mV, followed by BQ221 with a ΔE_p of 130 ± 10.2 mV and then by the commercially available Dropsens SPCE with a ΔE_p of 167 ± 30.5 mV. Carbon paste 7105 performed the worst with a ΔE_p of 203 ± 13.3 mV. Subsequently, it was decided that carbon paste BQ242 would be utilised for further experiments in the assay development.

Electrochemical sensor performance is affected by the surface area of the electrode. Increased surface roughness can lead to an increase in the effective surface area of the device and hence improved performance. The surface roughness of the manufactured carbon electrodes and a commercially available

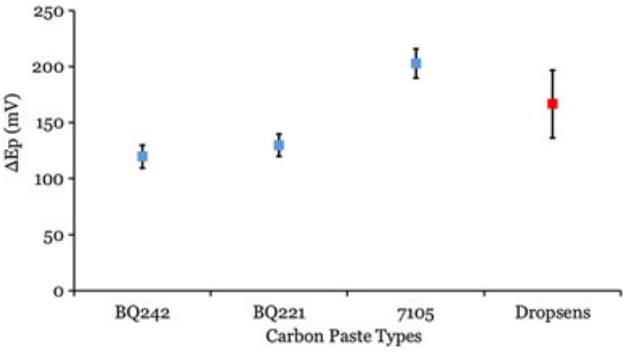

Figure 4. Graphical representation of the electrochemical characterisation via cyclic voltammetry of different DuPont carbon pastes and Dropsens SPCE. Cyclic voltammetry's were recorded at a scan rate of 50 mV s^{-1} in the presence of the redox pair $Fe(CN)_6^{3-/4-}$ (10 mM in phosphate buffer), and the average peak separation between the observed oxidation and reduction potentials (ΔE_p) were recorded as a function of the electrode surface. Error bars represent standard deviation (n = 10).

Dropsens DRP-C1110 sensor was measured using a Dektak 3 profilometer. These measurements were taken at the four locations across the surface of the carbon layers of five different manufactured and commercial devices as numbered in Figure 5. Both electrodes were treated prior to measurement using chronoamperometric cleaning as detailed previously.

There was little variation in median surface roughness between the measurement locations for the Dropsens electrodes compared with that of the carbon electrodes as shown in Figure 6. However, overall the measured surface roughness of the carbon electrodes was higher, which may be a contributing factor in the improved electrochemical performance shown in Figure 4. Scanning electron microscopy observation was also carried out to further investigate the cause of surface roughness variation exhibited by the carbon electrodes. As can be seen in Figure 7, the carbon particles of the electrodes are larger in size and packed together in such a way to form holes into the layer at the surface. The carbon particles that constitute the equivalent layer in the Dropsens electrodes DRP-C1110 are

Table 2. Showing oligonucleotide sequences used in the study.

Item	ID	Sequence (5'-3')
bla$_{NDM}$ specific probe	P7	GTGCTGCCAGACATTCGGTG-Lys(AEEEA)-C12A
Synthetic oligonucleotide *bla*$_{NDM}$ complement	P7C	CACCGAATGTCTGGCAGCAC
Synthetic oligonucleotide Negative Control	N	TGGTATGTGGAAGTTAGATTGGGATCA

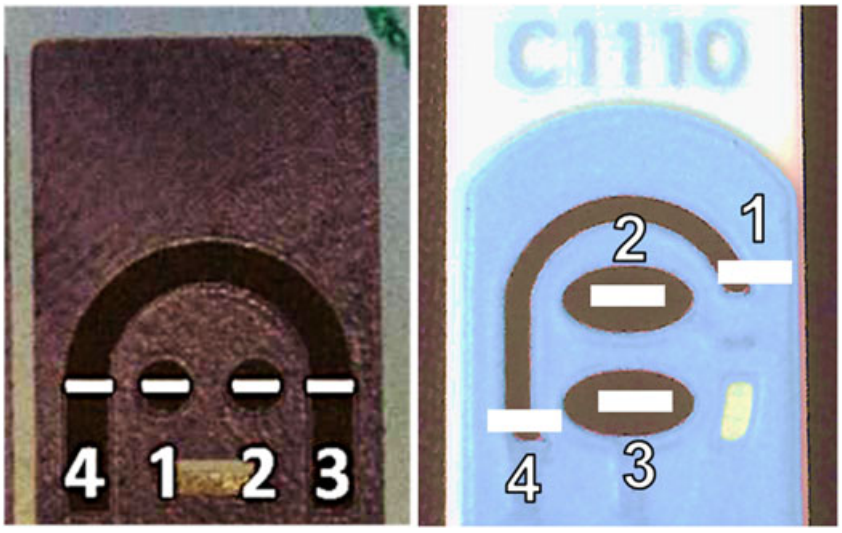

Figure 5. Surface roughness measurement locations for carbon electrode (left) and DropSens electrodes (right).

finer and more densely packed with no signs of holes at the surface layer. The morphology of the carbon film on the LTCC-based screen-printed electrodes leads to a larger effective surface area that contributes to improved electrochemical performance.

Effect of the dielectric paste

Three different Gwent dielectric insulation materials (D5, D1, and P2) were tested in terms of unspecific DNA binding and hydrophobicity of the dielectric surface. Both factors are important when immobilising and attaching analytical probes such as PNA or antibodies to the electrode surface. During the probe immobilisation process, individual working electrodes are covered with droplets of various probe solutions. If the dielectric is too hydrophilic, there is a risk that the droplet of solution containing the functionalising elements would not remain on the working electrode surface for required incubation time to properly affix the probes on to the electrode surface. Accordingly in Table 3, the contact angle measurements of the three Gwent dielectrics showed that material D1 was

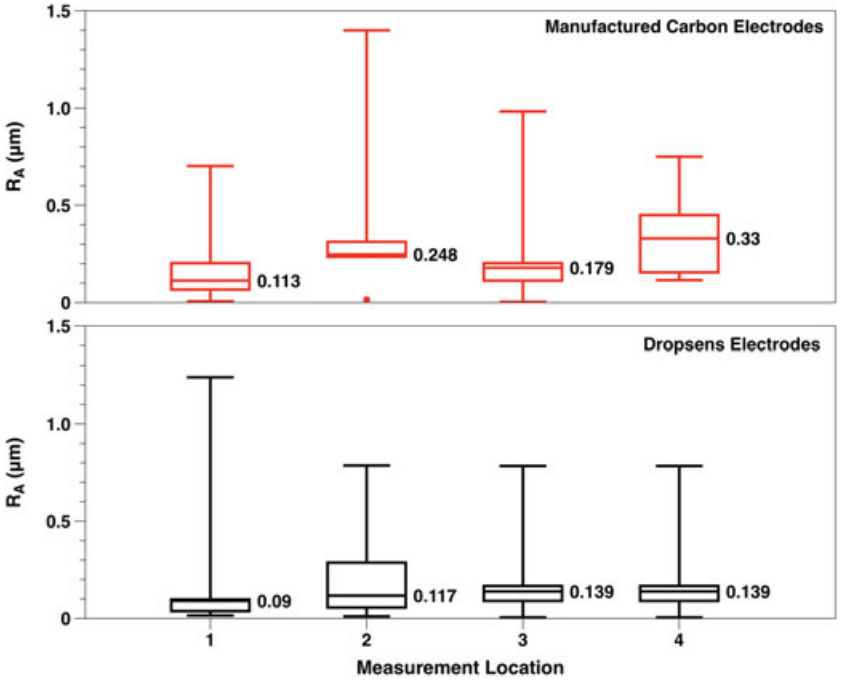

Figure 6. Comparison of average surface roughness measurements of DropSens and carbon electrodes.

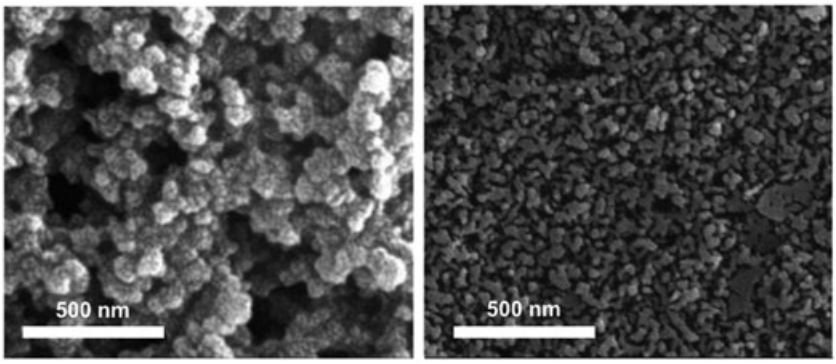

Figure 7. Scanning electron microscope images of carbon layer electrodes: (left) Low Temperature Co-fired Ceramics-based electrodes and (right) DropSens electrodes.

significantly more hydrophilic than D5, P2, and the dielectric used in the Dropsens DRP-C1110 electrodes.

Additionally, to better qualify the dielectric materials, unspecific binding of fluorescence (Cy3)-labelled DNA oligonucleotides on three different Gwent dielectric materials was tested with a Tecan LS Reloaded fluorescence scanner. As shown in Figure 8, there was a high degree of unspecific DNA binding on P2, no detectable binding on D1, and only a small degree of DNA binding on D5. Also, to verify the findings, control experiments were run with different lengths of Cy3-labelled oligonucleotides (1 mer, 20 mer, and 40 mer) to confirm that the unspecific binding on the dielectric materials was unique to the oligonucleotide chains adsorbing on to the dielectric material and not the fluorescence dye, as shown in Figure 9. Based on the DNA binding study and contact angle measurements, Gwent paste D5 was selected to produce the insulation layer.

Functionalisation of screen-printed carbon electrode with peptide nucleic acid probes

Screen-printed carbon electrode sensors were functionalised with amino-modified PNA probes (*bla*$_{NDM}$ variant) by electrografting via in situ generated diazonium cations from an in-house modified protocol. (Eissa and Zourob, 2012) The individual surface modification steps were confirmed by EIS measurements in 2 mM Fe $[CN]_6^{3-/4-}$solution in 1 mM KCl solution. As shown in Figure 10A, the black curve shows the signal obtained from bare fabricated LTCC-based SPCEs. Binding of 4-carboxyphenyl to the electrode surface caused a large signal (impedance) increase shown by the red curve resulting from the addition of negative charges on the surfaces from the carboxyl groups which interact with the negatively charged $Fe[CN]_6^{3-/4-}$ redox active species in solution. Activation of the 4-carboxyphenyl groups (AP film) by binding EDC in a solution with NHS in MES buffer at pH 5.0 resulted in a significant depreciation of the impedance signal shown by the blue curve, with a small electron charge transfer resistance value These values were obtained by fitting the EIS spectra curves to a Randles equivalent circuit, which was automatically generated by the Autolab NOVA analysis software. The depreciation of the impedance signal (blue curve) was caused by the EDC and NHS induced nullification of the carboxyl groups and its negative charges on the electrode surface. (Conde et al., 2014; Sam et al., 2010) After covalent attachment of the amino-modified PNA probes to the NHS activated ester group the R_{CT} value showed a slight impedance increase as shown by the bright green curve. An initial evaluation of the LTCC SPCE functionalisation process was undertaken. As demonstrated in Figure 10B, the *bla*$_{NDM}$-specific PNA probe P7, at a concentration of 10 μM, was initially examined with a short synthetic DNA target (20 μM) directly complementary to the probe sequence. The applied EIS setup enabled the direct, label-free detection of target hybridisation to the immobilised probe. EIS measurements obtained before (red curves) and after target addition (blue curves) allowed the hybridisation (significant change in spectra) to be monitored for a duration of 50 min over the course of subsequent EIS spectra measurements, with each spectrum plotted as a Nyquist plot to capture charge transfer

Table 3. Contact angle measurements of the three Gwent dielectric pastes ($n = 6$).

Dielectric material	Contact angle (°)
D2020823P2	90.9 (±2.2)
D2070423D5	89.1 (±2.3)
D2071120D1	63.9 (±5.1)
Dropsens DRP-C1110	95.4 (±3.5)

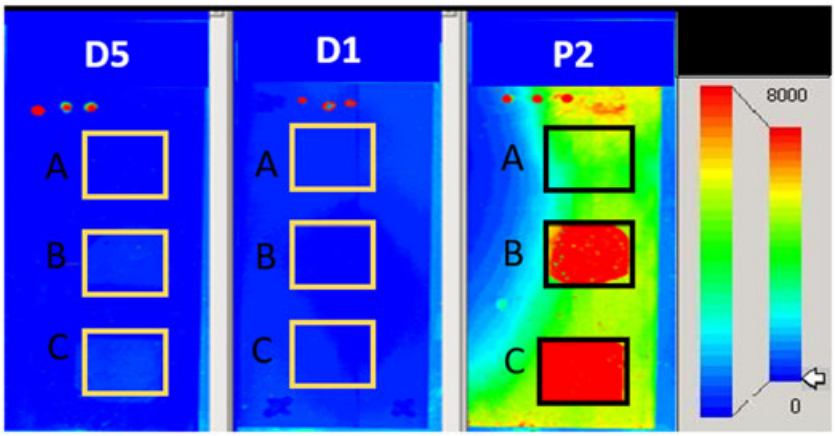

Figure 8. Fluorescent evaluation of unspecific Cy3-labelled DNA oligonucleotides binding on three different dielectric materials (from left to right: D5, D1, and P2). As observed, there was a high degree of unspecific DNA binding on material P2, with no detectable DNA binding on material D1 and a small degree of binding on material D5. Cy3-labelled DNA oligonucleotides were used at varying concentrations (A) 2x saline sodium citrate buffer (SSC), (B) 100 nM DNA oligonucleotides in SSC, and (C) 2 μM DNA oligonucleotides in SSC.

resistance values R_{CT}. However, as shown in Figure 10C, functionalised LTCC SPCEs without PNA probes, that is, negative control, showed no changes in the EIS spectra before (red curves) and after target addition (blue curves).

For subsequent EIS experiments a signal increase ratio, dR_{CT}, was defined as the R_{CT} value obtained post-hybridisation (52 min after target addition, respectively, the 10th consecutive EIS measurement after target addition) divided by the R_{CT}, the pre-hybridisation value for a particular concentration of DNA target. Similar approaches representing hybridisation induced impedimetric increases have been employed in other publications. (Huang et al., 2015; Kafka et al., 2008; Peng et al., 2007)

In developing a sensitive and specific bla_{NDM} EIS assay, parameters pertaining to the functionalisation of SPCEs were considered. Finding the optimal immobilised probe concentrations that facilitated enhanced EIS signal detection was of primary concern. To evaluate this, various concentrations of amino-modified PNA probes, that is, 2, 5, and 10 μM were immobilised on the both LTCC-based and Dropsens SPCEs, and the EIS response after incubation with 20 μM complimentary DNA targets for 52 min were recorded. For these set of experiments 50 mM NHS with

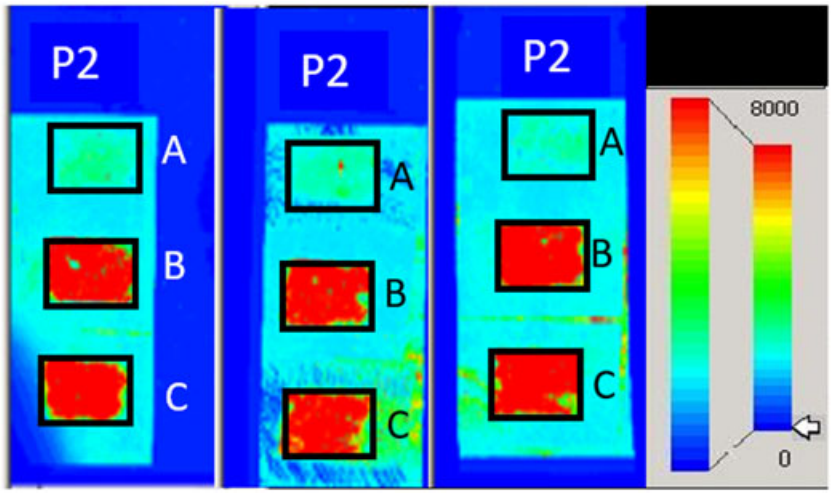

Figure 9. Fluorescent control evaluations of unspecific Cy3-labelled DNA oligonucleotides binding on three different 3 replicate samples of P2 dielectric material. Panels A, B, and C were each incubated with solutions containing 2 μM of 1, 20, and 40 mer Cy3-labelled DNA oligonucleotides, respectively. After which, the surfaces were rinsed, dried, and measurements taken

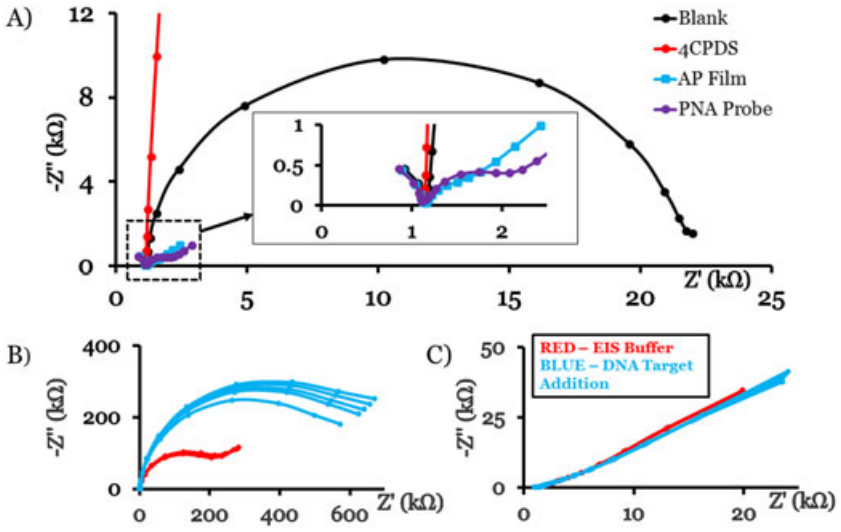

Figure 10. Electrochemical impedance spectroscopy spectra of screen-printed carbon electrode (SPCE) functionalization and characterisation in EIS buffer containing 1 mM KCl with 2 mM $Fe[CN]_6^{3-/4-}$, unless stated otherwise. (A) EIS spectra following the SPCE functionalization process, starting with a blank SPCE (black), in situ generated 4-carboxyphenyl diazonium salts were generated and electrografted on to the SPCE surface (red), then see inset; 4-carboxyphenyl/AP film was activated by incubating the SPCE in EDC and NHS (blue), and subsequently 20 μM of amino-modified peptide nucleic acid (PNA) probes (purple) were functionalised on to the SPCE surface, and the electrodes were ready for running. (B) EIS spectra of functionalised SPCE response with 10 μM PNA probes after incubation in solution containing 20 μM complementary target DNA for 50 min. (C) EIS spectra of PNA-free SPCE (negative control) after incubation in solution containing 20 μM complementary target DNA for 50 min. NB: all the other functionalisation steps were undertaken except incubating the SPCE in amino-modified PNA probes.

200 mM EDC, in 100 mM MES buffer (pH 5.0) was used to activate the terminal carboxyl groups (AP film) on the electrode surface. As seen in Figure 11A, while there were no discernible patterns of the EIS assay response to the concentration of immobilised probes, LTCC-based SPCEs with 10 μM amino-modified probes were observed to be more sensitive than other SPCEs with an average $dR_{CT} = 2.78$. Interestingly, under the current functionalisation conditions, Dropsens SPCEs were the least sensitive to the functionalisation conditions.

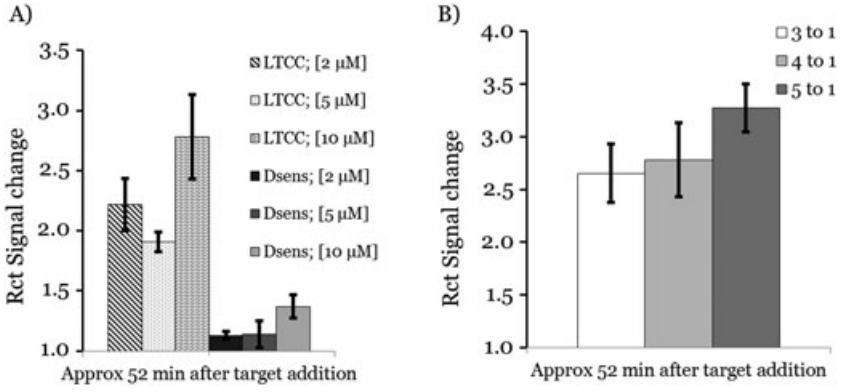

Figure 11. Images characterising the effects of key functionalisation steps on electrochemical impedance spectroscopy assay sensitivity. (A) Comparison of the response of functionalised fabricated LTCC SPCEs against Dropsens SPCEs in the presence of varying concentrations of amino-modified peptide nucleic acid (PNA) probes at 2, 5, and 10 μM after incubation with 20 μM complimentary DNA targets for 52 min. (B) LTCC SPCEs functionalised with 10 μM PNA probes were incubated in 20 μM complimentary target DNA for 52 min, while the optimal concentration of EDC/NHS used to activate the AP film during the functionalisation process was evaluated. A constant concentration of 50 mM NHS was used while EDC was varied at three concentrations (i.e., 150, 200 and 250 mM), and using EDC at 250 mM was shown to be the optimal concentration for the best assay sensitivity. All concentrations of EDC/NHS were mixed in 100 mM MES buffer (pH 5.0). NB: Error bars indicate standard deviation ($n = 4$).

Another critical parameter for the functionalisation process is the effect of the cross-linking agents used in anchoring the probes onto the SPCE surface particularly EDC and NHS. EDC is a well known zero-length cross-linking agent utilised in coupling carboxyl or phosphate groups to primary amines and has been used extensively in diverse applications. (Mol et al., 2010; Sam et al., 2010) One of the main advantages of EDC coupling is its water solubility, which allows direct bioconjugation without prior organic solvent dissolution. However, the coupling reaction has to be carried out fast, as the reactive ester that is formed can be rapidly hydrolysed in aqueous solutions. To increase the stability of this active ester, NHS can also be introduced into the mixture. The addition of NHS stabilises the amine-reactive intermediate by converting it to an amine-reactive NHS ester, thus increasing the efficiency of EDC-mediated coupling reactions. Subsequently, critical parameters that should be controlled when using EDC are threefold: the pH as the hydrolysis is largely dependent on it; the amount of EDC so that nucleic acids do not aggregate because of loss of electrostatic repulsive forces among them and the EDC/NHS ratio. (Liu et al., 2013; Sam et al., 2010; Sehgal and Vijay, 1994) In this study, the efficiency of the surface carbodiimide coupling reaction was monitored by observing the changes in EIS assay sensitivity in response to various EDC/NHS concentrations.

An extensive literature review showed a lack of consensus on the concentrations of EDC/NHS for optimal activation of surface carboxylic acids with reports ranging from a few micromolar to 0.4 M. (Booth et al., 2011; Liu et al., 2013; Mol et al., 2010; Sam et al., 2010) However, in keeping with unpublished data from our laboratory and literature under similar conditions, the efficiency of the AP film activation was evaluated using NHS at a constant concentration of 50 mM, while EDC was used at three concentrations, that is, 150, 200, and 250 mM, all in 100 mM MES buffer at pH = 5.0. The EIS response of LTCC SPCEs functionalised with 10 μM PNA probes and incubated with 20 μM complimentary target DNA for 52 min were recorded. As shown in Figure 11B, there is a positive correlation between increasing EDC concentration and EIS assay sensitivity, with electrodes functionalised using EDC at 250 mM showing the best sensitivities with an average $dR_{CT} = 3.27$.

Consequently, after establishing the standard functionalisation conditions of LTCC SPCEs as immobilising 10 μM PNA probes and activating the AP film using 250 mM EDC with 50 mM NHS in 100 mM MES buffer (pH 5.0). Figure 12 shows the standard curve, which was established based on the dR_{CT} after 60 and 52 min after target addition. The limit of detection of hybridisation of a synthetic oligonucleotide to immobilised PNA probes, defined as the buffer negative control signal plus three times the standard deviation, was determined to be 200 nM. The error bars in Figure 12 represent the standard deviation of the signal increase ratios obtained from four individual biosensors tested with each target concentration. The mean relative standard deviation (RSD) obtained over a concentration range from 100 nM to 20 μM was 10%. This level of reproducibility of technical replicates obtained with different functionalised biosensors, which were tested with the same target solutions, are in good agreement with previously published EIS biosensors on gold electrodes (Corrigan et al., 2012; Henihan et al., 2016) and even higher compared with RSD values of functionalised gold electrodes tested with the same probe/target couple. We previously obtained a mean RSD of 14% with the same NDM-specific PNA probe sequence immobilised on gold screen-printed electrodes through a self-assembled monolayer which were tested with the same target oligonucleotide as used herein. (Huang et al., 2015)

Additionally, as shown in Figure 13, the specificity of the functionalised LTCC SPCEs (dark grey) was evaluated. Only around 41% cross-reactivity was demonstrated against PNA probe-free electrodes (light grey) and 25% cross-reactivity against noncomplementary oligo targets (white). For this experiment, 20 μM target concentrations were used for each analysis, after incubation with electrodes for 52 min. These data confirm good specificity of the functionalised carbon EIS biosensors with hybridisation reactions performed at room temperature and without an additional washing step after hybridisation, thus under non-stringent hybridisation conditions. Hybridisation with a high target concentration of 20 μM caused only a signal increase ratio of 1.6, which was only marginally higher than the buffer control baseline value of 1.2. If there is a requirement to further enhance the specificity of the assay, for example, if single nucleotide polymorphism (SNP) specificity would be required for a specific application, the hybridisation conditions of the EIS test can be adopted by enhancing the stringency of the hybridisation conditions. We have shown previously that the specificity of EIS-based assays can be enhanced by applying a more stringent hybridisation buffer. This

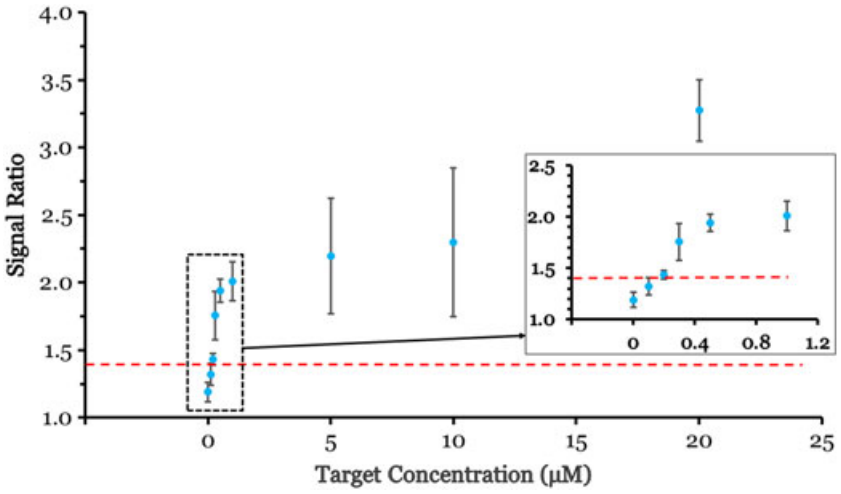

Figure 12. Dose-response curve of functionalised LTCC SPCE after 52 min of incubation with target DNA. Functionalised LTCC SPCEs with 10 μM peptide nucleic acid probes were evaluated against a range of complimentary target DNA concentrations (0–20 μM). See inset at lower target concentration, 3-σ analysis (red line indicates cut-off point) confirmed the limit of detection of the LTCC SPCE at 200 nM of target DNA. During the functionalisation process, AP film was activated using 250 mM of EDC with 50 mM of NHS in 100 mM MES buffer at pH = 5.0. Error bars indicate standard deviation ($n = 4$).

was achieved by adding 50% formamide to EIS buffer. (Huang et al., 2015) Furthermore, the use of PNA probes instead of DNA probes have been shown to be beneficial for SNP discrimination through preferential binding of fully complementary target sequences over those with a SNP. (Lao et al., 2009; Ratilainen et al., 2000) Moreover, the specificity of the EIS assay could further be enhanced by applying an elevated temperature close to the melting temperature of the probe/target complex during the hybridisation as usually applied, for example, in DNA microarray experiments. (Leinberger et al., 2010)

As observed in the results previously, the efficiency of the EIS assay using LTCC SPCEs was somewhat lacking in comparison with EIS tests performed previously with Dropsens screen-printed gold electrodes functionalised with 1.5 μM thiol modified bla_{NDM} PNA probes for the detection of the same synthetic targets but with a slightly lower limit of detection of 10 nM (10×10^{-9}M) and subsequently direct, amplification-free detection from a bla_{NDM} -harbouring plasmid. (Huang et al., 2015)

However, several advantages of carbon pastes over gold for sensing applications have been documented extensively in the literature. Carbon pastes are relatively

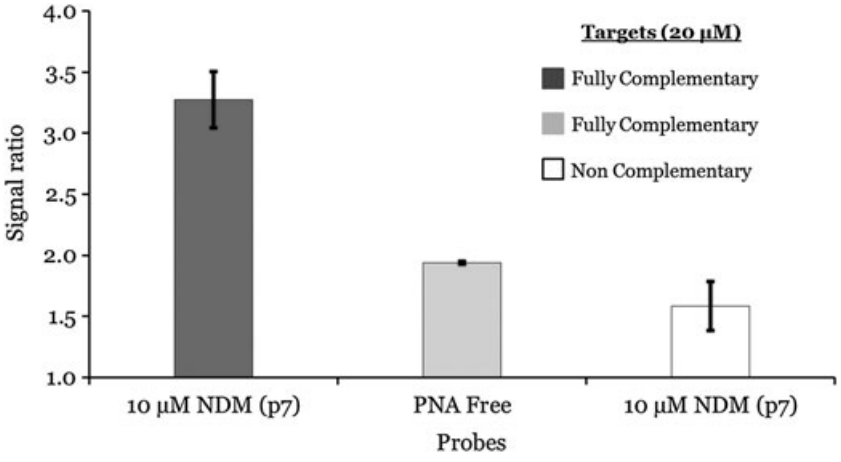

Figure 13. Graphs evaluating the specificity of LTCC SPCEs after incubation with target DNA for 52 min. Using an LTCC SPCE with 10 μM NDM (p7) probe and 20 μM NDM7 DNA target concentration as the benchmark (dark grey), PNA-Free SPCEs with 20 μM NDM7 DNA target showed across 41% cross-reactivity (light grey), additionally in keeping the benchmark probe but replacing the target with 20 μM non-complementary DNA target showed ~25% cross reactivity (white).

inexpensive, lead to low background currents and possess a wide potential range, thereby making them ideal for the manufacturing of sensing platforms. (Wang et al., 1996; Wang et al., 1998) Our study highlights also another significant benefit of using carbon inks over gold, with respect to the probe functionalisation process for the EIS-based molecular diagnostics of nucleic acid targets. As shown in Table 4, which compares the process steps involved in the functionalisation of carbon electrodes with a common gold electrode functionalisation protocol (Corrigan et al., 2012; Corrigan et al., 2013), gold electrode functionalisation is based on SAM formation of gold-thiol bonds. This process requires an extremely clean gold surface in order to generate well-structured, homogenous SAMs and is very time consuming, requiring 16 h for the formation of well-structured SAMs. In comparison, the newly developed functionalisation protocol for PNA probes on carbon electrodes does not require the carbon surface to be cleaned extensively before functionalisation. In contrast to the covalent attachment of the amino-modified PNA probes, thiol-modified PNA probes are bound to gold in SAMs via chemisorption creating only a less stable semi-covalent linkage. And finally, the overall process for producing PNA functionalised carbon electrodes takes 2 h 40 min compared with 17 h 30 min on gold electrodes. The development of reliable carbon electrodes for EIS-based sensors can therefore be an inexpensive and effective alternative to gold electrodes. The higher stability of the covalent attachment of the PNA probes on carbon electrodes is also anticipated to have a positive impact on the storage stability of the functionalised carbon electrodes. Long-term storage of functionalised gold screen-printed electrodes for EIS-based molecular diagnostics applications is a difficult task as EIS measurements employing probe layers of self-assembled monolayers of a mixture of thiolated probes and mercaptohexanol require well-structured, homogenous monolayers. (Ricci et al., 2009) Dry storage of such electrodes followed by rehydration before the EIS measurement comprises the risk of the introduction of disturbances into these well-structured self-assembled monolayers and thus may have a negative impact on the EIS response of such biosensors. The use of ternary SAMs of a mixture of thiolated probes, mercaptohexanol, and 1,6-hexanedithiol has been described with enhanced long term dry storage stability. (Kuralay et al., 2012; Miodek et al., 2015) Electrochemical biosensors applying DNA probes covalently attached to carbon electrodes have been described with prolonged storage stability. (Mazloum-Ardakani et al., 2016; Ruffien et al., 2003) A differential pulse voltammetry biosensor with DNA probes covalently bound to glassy carbon electrodes, for example, showed no loss of sensitivity after 10 days storage in buffer at 4 °C. (Amouzadeh Tabrizi and Shamsipur, 2015) Ulianas *et al*. reported a storage stability of 45 days for an electrochemical biosensor with amino-modified DNA probes covalently attached to succinimide groups of acrylic microspheres when stored in phosphate buffer at 4 °C. (Ulianas et al., 2014) For a successful real world application of electrochemical nucleic acid biosensors batch production of functionalised biosensors followed by long-term dry

Table 4. Process steps involved in functionalisation of gold and carbon electrodes and time requirements.

	Gold electrodes		Carbon electrodes	
	Method	Time	Method	Time
Cleaning	CV cycling in 0.1 M H_2SO_4	30 min	-	-
Surface modification	-	-	Electrochemical reduction of in situ generated 4-carboxyphenyl diazonium salt	10 min
Surface activation	-	-	Carbodiimide chemistry (EDC/NHS)	60 min
Probe immobilisation	Incubation with thiol-modified PNA probes in 50% DMSO Gold-thiol bond formation (SAM)	16 h	Incubation with amino-modified PNA probes in PBS (pH 7.4) Covalent probe attachment	60 min
Blocking	1 mM mercaptohexanol	60 min	1% (v/v) ethanolamine	30 min
Total time for electrode functionalisation	17 h 30 min		2 h 40 min	

storage ideally at room temperature is desirable if not essential for a successful market entry. To fully achieve this goal, further dedicated studies are required. The higher stability of PNA probes which we use in our assay instead of commonly used DNA probes exhibits a significant advantage regarding the development of a stable EIS biosensor with long-term storage capability. PNA is chemically stable and is resistant to hydrolytic cleavage by nucleases or proteases. (Siddiquee et al., 2015)

Conclusions

We successfully produced low-cost carbon LTCC electrochemical sensors for use in molecular detection of nucleic acids. Improved sensor sensitivity was achieved by selection of the dielectric material based on low unspecific DNA binding and low wettability. The best and finally used sensors were produced using BQ242 carbon paste from DuPont in conjunction with dielectric paste D5 from Gwent. Under the conditions of our study, these sensors demonstrated superior performance to commercially available carbon electrodes. The carbon electrodes were functionalised with PNA probes using a new protocol for covalent probe attachment, which was over six times faster than previous protocols used for gold electrodes. These functionalised sensors showed dose-dependent signals in kinetic EIS measurements of synthetic bla_{NDM} targets as a proof of concept study for rapid antimicrobial resistance detection. This work represents to the best of our knowledge the first example of an EIS-based label-free molecular detection for nucleic acid targets using carbon screen-printed electrodes with immobilised PNA probes. The excellent molecular detection performance combined with a low cost and accelerated sensor manufacturing and functionalisation process make our system a very attractive platform for further molecular targets serving the unmet need for rapid detection of antimicrobial resistance at POC at competitive costs.

Acknowledgments

Part of this work was funded by Scottish Sensor Systems Centre, now Scottish Innovation Centre for Sensor and Imaging Systems under the grant number 20130219_Molnlycke with the title “Carbon Screen Printed Electrodes for Label Free Molecular Diagnostics”. The authors would also like to acknowledge the financial support of the Innovative electronic Manufacturing Research Centre through the flagship project “Smart Microsystems”, reference FS/01/02/10. We also would like to thank Russell McCraith, MHC Scotland Ltd., for commercial advice during the project.

REFERENCES

Amouzadeh Tabrizi, M., and M. Shamsipur. **2015**. A label-free electrochemical DNA biosensor based on covalent immobilization of salmonella DNA sequences on the nanoporous glassy carbon electrode. Biosensors and Bioelectronics *69*:100–105.

Booth, M. A., S. Harbison, and J. Travas-Sejdic. **2011**. Development of an electrochemical polypyrrole-based DNA sensor and subsequent studies on the effects of probe and target length on performance. Biosensors and Bioelectronics *28*:362–367.

Carrer, A., N. Fortineau, and P. Nordmann. **2010**. Use of ChromID extended-spectrum beta-lactamase medium for detecting carbapenemase-producing Enterobacteriaceae. J Clin Microbiol *48*:1913–4.

CDC. **2013**. Antibiotic Resistance Threats in the United States. Centers for Disease Control and Prevention, U.S.

Cederquist, K. B., and S. O. Kelley. **2012**. Nanostructured biomolecular detectors: pushing performance at the nanoscale. Current Opinion in Chemical Biology *16*:415–421.

Ciani, I., H. Schulze, D. K. Corrigan, G. Henihan, G. Giraud, J. G. Terry, A. J. Walton, R. Pethig, P. Ghazal, J. Crain, C. J. Campbell, T. T. Bachmann, and A. R. Mount. **2012**. Development of immunosensors for direct detection of three wound infection biomarkers at point of care using electrochemical impedance spectroscopy. Biosens Bioelectron *31*:413–8.

Conde, J., J. T. Dias, V. Grazú, M. Moros, P. V. Baptista, and J. M. De La Fuente, **2014**, Revisiting 30 years of biofunctionalization and surface chemistry of inorganic nanoparticles for nanomedicine: Frontiers in Chemistry, *2*.

Corrigan, D. K., H. Schulze, G. Henihan, I. Ciani, G. Giraud, J. G. Terry, A. J. Walton, R. Pethig, P. Ghazal, J. Crain, C. J. Campbell, A. R. Mount, and T. T. Bachmann. **2012**. Impedimetric detection of single-stranded PCR products derived from methicillin resistant staphylococcus aureus (MRSA) isolates. Biosens Bioelectron *34*:178–84.

Corrigan, D. K., H. Schulze, G. Henihan, A. Hardie, I. Ciani, G. Giraud, J. G. Terry, A. J. Walton, R. Pethig, P. Ghazal, J. Crain, C. J. Campbell, K. E. Templeton, A. R. Mount, and T. T. Bachmann. **2013**. Development of a PCR-free electrochemical point of care test for clinical detection of methicillin resistant Staphylococcus aureus (MRSA). Analyst *138*:6997–7005.

ECDC, **2011**, Risk assessment on the spread of carbapenemase-producing enterobacteriaceae (CPE) through patient transfer between healthcare facilities, with special emphasis on cross-border transfer, european centre for disease prevention and control.

Eissa, S., and M. Zourob. **2012**. A graphene-based electrochemical competitive immunosensor for the sensitive detection of okadaic acid in shellfish. Nanoscale *4*:7593–7599.

Farber, J., K. A. Moder, F. Layer, I. Tammer, W. Konig, and B. Konig. **2008**. Extended-spectrum beta-lactamase detection with different panels for automated susceptibility testing and with a chromogenic medium. J Clin Microbiol *46*:3721–7.

Fomda, B. A., A. Khan, and D. Zahoor. **2014**. NDM-1 (New Delhi metallo beta lactamase-1) producing Gram-negative bacilli. Emergence & clinical implications: The Indian Journal of Medical Research *140*:672–678.

Fosheim, G. E., R. B. Carey, and B. M. Limbago. **2007**. Evaluation of the AdvanDx VRE EVIGENE assay for detection of vanA in vancomycin-resistant Staphylococcus aureus. J Clin Microbiol *45*:1611–3.

Gebala, M., L. Stoica, S. Neugebauer, and W. Schuhmann. **2009**. Label-free detection of DNA hybridization in presence of intercalators using electrochemical impedance spectroscopy. Electroanalysis *21*:325–331.

Gongora-Rubio, M. R., P. Espinoza-Vallejos, L. Sola-Laguna, and J. J. Santiago-Avilés. **2001**. Overview of low temperature co-fired ceramics tape technology for meso-system technology (MsST). Sensors and Actuators A: Physical *89*:222–241.

Grieshaber, D., R. MacKenzie, J. Vörös, and E. Reimhult, **2008**, Electrochemical biosensors – sensor principles and architectures: sensors (Basel, Switzerland), *8*, p. 1400–1458.

Hawkey, P. M. **2015**. Multidrug-resistant Gram-negative bacteria: a product of globalization. Journal of Hospital Infection *89*:241–247.

Henihan, G., H. Schulze, D. K. Corrigan, G. Giraud, J. G. Terry, A. Hardie, C. J. Campbell, A. J. Walton, J. Crain, R. Pethig, K. E. Templeton, A. R. Mount, and T. T. Bachmann. **2016**. Label- and amplification-free electrochemical detection of bacterial ribosomal RNA. Biosensors and Bioelectronics *81*:487–494.

Huang, J. M., G. Henihan, D. Macdonald, A. Michalowski, K. Templeton, A. P. Gibb, H. Schulze, and T. T. Bachmann. **2015**. Rapid electrochemical detection of New Delhi metallo-beta-lactamase genes to enable point-of-care testing of carbapenem-resistant enterobacteriaceae. Analytical Chemistry *87*:7738–7745.

Ibáñez-García, N., J. Alonso, C. S. Martínez-Cisneros, and F. Valdés. **2008**. Green-tape ceramics. New technological approach for integrating electronics and fluidics in microsystems: TrAC Trends in Analytical Chemistry *27*:24–33.

Jean, S.-S., W.-S. Lee, C. Lam, C.-W. Hsu, R.-J. Chen, and P.-R. Hsueh, **2015**, Carbapenemase-producing gram-negative bacteria: current epidemics, antimicrobial susceptibility and treatment options: future microbiology, *10*, p. 407–425.

Kaase, M., F. Szabados, L. Wassill, and S. G. Gatermann. **2012**. Detection of carbapenemases in Enterobacteriaceae by a commercial multiplex PCR. J Clin Microbiol *50*:3115–8.

Kafka, J., O. Pänke, B. Abendroth, and F. Lisdat. **2008**. A label-free DNA sensor based on impedance spectroscopy. Electrochimica Acta *53*:7467–7474.

Kay, R. W., and M. P. Y. Desmulliez. **2012**. A review of stencil printing for microelectronic packaging. Soldering & Surface Mount Technology *24*:38–50.

Kumarasamy, K. K., M. A. Toleman, T. R. Walsh, J. Bagaria, F. Butt, R. Balakrishnan, U. Chaudhary, M. Doumith, C. G. Giske, S. Irfan, P. Krishnan, A. V. Kumar, S. Maharjan, S. Mushtaq, T. Noorie, D. L. Paterson, A. Pearson, C. Perry, R. Pike, B. Rao, U. Ray, J. B. Sarma, M. Sharma, E. Sheridan, M. A. Thirunarayan, J. Turton, S. Upadhyay, M. Warner, W. Welfare, D. M. Livermore, and N. Woodford. **2010**. Emergence of a new antibiotic resistance mechanism in India. Pakistan, and the UK: a molecular, biological, and epidemiological study: Lancet Infect Dis *10*:597–602.

Kuralay, F., S. Campuzano, and J. Wang. **2012**. Greatly extended storage stability of electrochemical DNA biosensors using ternary thiolated self-assembled monolayers. Talanta *99*:155–160.

Lacrotte, Y., J. P. Carr, R. W. Kay, and M. P. Y. Desmulliez. **2013**. Fabrication of a low temperature co-fired ceramic package using powder blasting technology. Microsystem Technologies *19*:791–799.

Lao, A. I. K., X. Su, and K. M. M. Aung. **2009**. SPR study of DNA hybridization with DNA and PNA probes under stringent conditions. Biosensors and Bioelectronics *24*:1717–1722.

Leinberger, D. M., V. Grimm, M. Rubtsova, J. Weile, K. Schröppel, T. A. Wichelhaus, C. Knabbe, R. D. Schmid, and T. T. Bachmann. **2010**. Integrated detection of extended-spectrum-beta-lactam resistance by DNA microarray-based genotyping of TEM. SHV, and CTX-M Genes: Journal of Clinical Microbiology *48*:460–471.

Lindholm-Sethson, B., J. Nyström, M. Malmsten, L. Ringstad, A. Nelson, and P. Geladi, **2010**, Electrochemical impedance spectroscopy in label-free biosensor applications: multivariate data analysis for an objective interpretation: analytical and bioanalytical chemistry, *398*, p. 2341–2349.

Linscott, A. J., and W. J. Brown. **2005**. Evaluation of four commercially available extended-spectrum beta-lactamase phenotypic confirmation tests. J Clin Microbiol *43*:1081–5.

Lisdat, F., and D. Schäfer. **2008**. The use of electrochemical impedance spectroscopy for biosensing. Analytical and Bioanalytical Chemistry *391*:1555–1567.

Liu, L., D. Deng, Y. Xing, S. Li, B. Yuan, J. Chen, and N. Xia. **2013**. Activity analysis of the carbodiimide-mediated amine coupling reaction on self-assembled monolayers by cyclic voltammetry. Electrochimica Acta *89*:616–622.

Mazloum-Ardakani, M., L. Hosseinzadeh, and M. M. Heidari, **2016**, Detection of the M268T Angiotensinogen A3B2 mutation gene based on screen-printed electrodes modified with a nanocomposite: application to human genomic samples: Microchimica Acta, *183*, p. 219–227.

Miodek, A., E. M. Regan, N. Bhalla, N. A. E. Hopkins, S. A. Goodchild, and P. Estrela, **2015**, Optimisation and characterisation of anti-fouling ternary SAM layers for impedance-based aptasensors: sensors (Basel, Switzerland), *15*, p. 25015–25032.

Mol, N. J., M. J. E. Fischer, and M. E. Fischer, **2010**, Amine coupling through EDC/NHS: a practical approach, surface plasmon resonance: methods in molecular biology, *627*, Humana Press, p. 55–73.

Naas, T., G. Cuzon, P. Bogaerts, Y. Glupczynski, and P. Nordmann. **2011**. Evaluation of a DNA microarray (Check-MDR CT102) for rapid detection of TEM, SHV, and CTX-M extended-spectrum beta-lactamases and of KPC, OXA-48, VIM, IMP, and NDM-1 carbapenemases. J Clin Microbiol *49*:1608–13.

Nordmann, P. **2010**. Résistance aux carbapénèmes chez les bacilles à Gram négatif. Med Sci (Paris) *26*:950–959.

O'Neill, J., **2014**, Antimicrobial resistance: tackling a crisis for the future health and wealth of nations, the review on antimicrobial resistance.

Park, J.-Y., and S.-M. Park, **2009**, DNA hybridization sensors based on electrochemical impedance spectroscopy as a detection tool: sensors, *9*, p. 9513–9532.

Peng, H., C. Soeller, N. A. Vigar, V. Caprio, and J. Travas-Sejdic, **2007**, Label-free detection of DNA hybridization based on a novel functionalized conducting polymer: selected papers from the ninth world congress on biosensors, *22*, p. 1868–1873.

Pesquero, N. C., M. R. Gongora-Rubio, and H. Yamanaka, **2013**, A novel LTCC electrochemical cell construction and characterization: a detection compartment for portable devices: Analyst, *138*, p. 4298–4304.

Ratilainen, T., A. Holmén, E. Tuite, P. E. Nielsen, and B. Nordén. **2000**. Thermodynamics of sequence-specific binding of PNA to DNA. Biochemistry *39*:7781–7791.

Reglier-Poupet, H., T. Naas, A. Carrer, A. Cady, J. M. Adam, N. Fortineau, C. Poyart, and P. Nordmann. **2008**. Performance of chromID ESBL, a chromogenic medium for detection of Enterobacteriaceae producing extended-spectrum beta-lactamases. J Med Microbiol *57*:310–5.

Ricci, F., N. Zari, F. Caprio, S. Recine, A. Amine, D. Moscone, G. Palleschi, and K. W. Plaxco. **2009**. Surface chemistry effects on the performance of an electrochemical DNA sensor. Bioelectrochemistry *76*:208–213.

Ruffien, A., M. Dequaire, and P. Brossier, **2003**, Covalent immobilization of oligonucleotides on p-aminophenyl-modified carbon screen-printed electrodes for viral DNA sensing: chemical communications, p. 912–913.

Sam, S., L. Touahir, J. Salvador Andresa, P. Allongue, J. N. Chazalviel, A. C. Gouget-Laemmel, C. Henry de Villeneuve, A. Moraillon, F. Ozanam, N. Gabouze, and

S. Djebbar. **2010**. Semiquantitative study of the EDC/NHS activation of acid terminal groups at modified porous silicon surfaces. Langmuir *26*:809–814.
Sehgal, D., and I. K. Vijay. **1994**. A method for the high efficiency of water-soluble carbodiimide-mediated amidation. Analytical Biochemistry *218*:87–91.
Siddiquee, S., K. Rovina, and A. Azriah. **2015**. A Review of Peptide Nucleic Acid: Advanced Techniques in Biology & Medicine, v.:3.
Suginta, W., P. Khunkaewla, and A. Schulte. **2013**. Electrochemical biosensor applications of polysaccharides chitin and chitosan. Chemical Reviews *113*:5458–5479.
Temkin, E., A. Adler, A. Lerner, and Y. Carmeli. **2014**. Carbapenem-resistant Enterobacteriaceae: biology, epidemiology, and management. Annals of the New York Academy of Sciences *1323*:22–42.
Ulianas, A., L. Y. Heng, M. Ahmad, H.-Y. Lau, Z. Ishak, and T. L. Ling. **2014**. A regenerable screen-printed DNA biosensor based on acrylic microsphere–gold nanoparticle composite for genetically modified soybean determination. Sensors and Actuators B: Chemical *190*:694–701.
Vasudev, A., A. Kaushik, K. Jones, and S. Bhansali. **2013**. Prospects of low temperature co-fired ceramic (LTCC) based microfluidic systems for point-of-care biosensing and environmental sensing. Microfluidics and Nanofluidics *14*:683–702.
Wang, J., M. Pedrero, H. Sakslund, O. Hammerich, and J. Pingarron. **1996**. Electrochemical activation of screen-printed carbon strips. Analyst *121*:345–350.
Wang, J., B. Tian, V. B. Nascimento, and L. Angnes. **1998**. Performance of screen-printed carbon electrodes fabricated from different carbon inks. Electrochimica Acta *43*:3459–3465.
Wilhelm, S., L. Y, K. R.W, and D. M.P.Y. **2012**. Novel Patterning Technologies for Ceramic MEMS. Microelectronics, Advancing.
Witte, C., and F. Lisdat. **2011**. Direct detection of DNA and DNA-ligand interaction by impedance spectroscopy. Electroanalysis *23*:339–346.